Mechanical Engineering Advances 2023; 1(1): 66.
Original Research Article

Theoretical analysis using thermal efficiency concept in straight micro channel printed circuit heat exchanger

Élcio Nogueira[1,*], Humberto Araújo Machado[1,2]

[1] *Faculdade de Tecnologia–FAT/UERJ, Resende 27537-000, Brazil*

[2] *Instituto de Aeronáutica e Espaço–IAE, São José dos Campos 12228-904, Brazil*

*** Corresponding author:** Élcio Nogueira, elcionogueira@hotmail.com

ARTICLE INFO

Received: 13 June 2023
Accepted: 14 July 2023
Available online: 21 August 2023

doi: 10.59400/mea.v1i1.66

ABSTRACT: The objective is to analyze the thermal and hydraulic performance in a micro channel straight printed circuit heat exchanger. Counterflow and parallel flow configurations were analyzed for water cooling using ethylene glycol-based fluid and platelet-shaped, non-spherical Boehmite alumina nanoparticles. The work presents results from applying a dimensionless theory that uses the concepts of thermal efficiency of heat exchangers and quantities associated with the second law of thermodynamics. Thermal efficiency, thermal effectiveness, thermal and viscous irreversibilities, thermodynamic Bejan number, and outlet water temperatures are presented in graph form. The data obtained allow us to conclude that the heat exchanger can work in a range of water and refrigerant flow rates below the design parameters. With the inclusion of nanoparticles with a volume fraction equal to 5.0%, the flow rates of the refrigerant fluid can be significantly reduced. The analysis performed shows that the use of nanoparticles improves the operational cost-benefit of the heat exchanger with a significant reduction in the hot water outlet temperature.

KEYWORDS: printed circuit heat exchanger (PCHE); microchannels; thermal efficiency; second law of thermodynamics; dimensionless theoretical analysis; non-spherical nanoparticles

1. Introduction

The work presents results from applying a dimensionless theory that uses the concepts of thermal efficiency of heat exchangers and quantities associated with the second law of thermodynamics. The influence of the refrigerant flow rate and the effect of the inclusion of non-spherical Alumina Boehmite nanoparticles on the thermohydraulic performance of a microchannel printed circuit heat exchanger are analyzed. The volume fraction of nanoparticles in the form of platelets corresponds to 5.0% of the volume of the refrigerant fluid, composed of 50% ethylene glycol. The fluid to be cooled is water at an initial temperature of 98 °C. The analysis method is dimensionless, and it applies the definition of thermal efficiency in heat exchangers and the second law of thermodynamics. Counter-flow and parallel-flow configurations were included in the analyses. A version of this article was presented at the 19th Brazilian Congress of Thermal Sciences and Engineering[1].

Seo et al.[2] performed performance tests on a micro-channel printed circuit heat exchanger (PCHE) in a single-phase regime. In counterflow and parallel flow configurations, Reynolds numbers ranged from 100 to 850. They developed empirical correlations for heat transfer coefficient and pressure drop as functions of the Reynolds number.

Rosa et al.[3] state inconsistencies between results published in recent decades for single-phase microscale heat transfer and that there is still no consensual model. They review experimental and numerical models available in the open literature. They clarify that scale effects, often insignificant in macro channels, can significantly influence the results and must be carefully considered. They call attention to measurement uncertainties due to their reduced characteristic dimensions. They analyze mathematical models for fluid dynamics and believe these should gain more interest because dimensional analyses migrate from microscale to nanoscale. They claim that correlations available for macro channels can be trusted at the microscale if all scale effects are negligible. However, simulations may be the only alternative for evaluating heat transfer rates when scale effects cannot be neglected.

Steinke and Kandlikar[4] clarify that the development of microchannels for heat exchangers and microfluidic devices depends on understanding the processes in these systems. In this sense, they compare experimental data to identify discrepancies between published works. They analyzed more than 150 works addressing flow and heat transfer aspects in microchannels, but approximately 40 were effectively valuable. The survey did not consider flow inlet and outlet regions, errors in channel geometry measurements, and experimental uncertainties. They concluded the need for more studies on heat transfer correlations for micro-channel heat exchangers. Despite this, the available data generally agree with the macro-scale theories. Therefore, they conclude that the classical theory applies to micro-channel and mini-channel flows.

Katz et al.[5] present a multilayer printed circuit heat exchanger prototype with 17 transparent plates photochemically bonded by diffusion. They measure pressure losses and heat transfer in zigzag flow geometry and the orientation of glued shims. Results are available in a dimensionless form to facilitate comparisons with thermo-hydraulic correlations. Two fluids with drastically different properties provide a unique method of exploring the effect of the working fluid on PCHE performance. Friction factor and Nusselt number were determined for laminar, transitional, and turbulent regimes spanning Reynolds number between 500 and 18,000. The friction factor shows an agreement of 10% and the heat transfer results of 15%, within the range of the tests performed. They end with an analysis of the thermo-hydraulic performance to establish a standard of comparison with other projects.

Baik et al.[6] developed a PCB exchanger design and analysis code to predict thermohydraulic performance. The range of Reynolds numbers considered corresponds to 2000–58,000. A prototype was manufactured to test the accuracy of the developed code. The experimental results demonstrated acceptable thermal performance and small pressure losses. The experimental results showed effectiveness above 90% in a small core of 200 mm. The code reproduced a similar performance. Regarding the pressure drop, they observe differences between experimental data and results obtained through the code, but they justify the difference by not including the losses located in the code.

Chai and Tassou[7] review and establish a comprehensive understanding of printed circuit heat exchangers (PCHEs). The study covered existing heat exchangers on the market and projects under development. They conclude that more work is needed to increase the range of applications for printed circuit heat exchangers. The work to be carried out must aim to optimize and develop new correlations that can reliably predict the performance of heat exchangers.

Zhao et al.[8] study a promising plate-type heat exchanger, the printed circuit (PCHE), of high compactness, suitable for high-pressure conditions. They investigate the thermohydraulic performance numerically of the heat exchanger using the SST k-ω turbulence model. They evaluate heat transfer and pressure loss and loss using Nusselt and Euler numbers. To define better-operating conditions, they

propose the Nu/Eu ratio for a comprehensive evaluation of the heat exchanger, considering thermal and hydrodynamic aspects. They conclude that thermal performance is better with higher mass flow and lower operating pressures.

Bhosale and Acharya[9] state that microchannels can be explored as turbine blades, rocket engines, hybrid vehicles, refrigeration cooling, thermal control in microgravity, and microgravity heat sink channels may be the solution to 21st-century cooling problems. They establish that the microchannel heat exchanger is more effective than the cross-fin and tube heat exchanger. It helps to reduce the amount of refrigerant in residential air conditioning systems. They advise those wishing to design a microchannel heat exchanger that the pressure loss and heat transfer characteristics must be accurately established. They state that the theoretical basis is not mature and that there is no uniform industry standard in manufacturing. They believe, however, that existing problems in manufacturing and applications will be resolved, and the microchannel heat exchanger will be widely used in industry.

Tang et al.[10] numerically analyze the effect of axial heat conduction on thermal performance in a zigzag-channel printed circuit heat exchanger (PCHE). The analysis includes Reynolds number, operating pressure, cold side inlet temperatures, and wall thermal conductivity. The results obtained indicate that axial heat conduction can significantly affect the thermal performance of PCHE at low Reynolds numbers but decreases at high Reynolds numbers for different working conditions. Furthermore, reducing the thermal conductivity of the wall can improve the thermal performance of the PCHE due to the influence of axial heat conduction on the partition wall.

Timofeeva et al.[11] experimentally investigate various alumina nanoparticles' thermal conductivity and viscosity in a fluid consisting of an equal amount of water and ethylene glycol. They develop a theoretical model for the analysis of experimental data. They claim that the presence of small fractions of nanoparticles significantly increases the viscosity of the suspension due to structural constraints. However, they demonstrate that the viscosity of alumina can be reduced by adjusting the pH of the nanofluid. They conclude that the use of alumina nanoparticles is of no benefit unless the viscosity of the nanofluid is diminished.

Monfared et al.[12] studied nanoparticle shape's effects on entropy generation in Boehmite alumina nanofluid flow in a double tube heat exchanger. Non-spherical nanoparticles are of the brick, sheet, platelet, and cylindrical type, suspended in a water and ethylene glycol mixture. Water flows from the annular side of the heat exchanger. The influence of the Reynolds number on the thermal and total entropy generation rates through the Bejan number was investigated numerically. The results obtained indicate that non-spherical nanoparticles in the form of platelets produce a lower rate of frictional entropy and that this increases with the increasing concentration of nanoparticles. The opposite occurs for the thermal entropy generation rate. They conclude that non-spherical nanoparticles in platelets have the best performance, and non-spherical nanoparticles have the worst performance.

To determine the thermal performance of different shapes of Boehmite Alumina compared to Al_2O_3 aluminum oxide, Nogueira[13] applied the second law of thermodynamics in a straight microchannel printed circuit heat exchanger. He concluded that the nanoparticles' shapes create greater thermal irreversibility and affect the interaction between the fluid base and the nanoparticles.

2. Methodology

Experimental data and specifications of the used heat exchanger were obtained from theoretical and experimental work prepared by Seo et al.[1]. The author performed thermal and dynamic performance

tests for a PCHE. The tests were carried out for configuration in counterflow, for Reynolds numbers in the range of 100–850, with inlet temperatures equal to 50° and 20°. Developed empirical correlations for the heat transfer coefficient as a function of the Reynolds number for both fluids, Equations (17) and (18).

Table 1 presents the properties of hot and cold fluids and Boehmite Alumina Platelet Nanoparticles.

Table 1. Fluid and nanoparticle properties, hot (Water), cold (Ethylene Glycol 50%), Boehmite Alumina platelets (Timofeeva et al.[11] and Monfared et al.[12]).

	ρ kg/m³	k W/ (m K)	Cp J/(kg K)	μ kg/(m s)	ν m/s²	α m/s²	Pr
Quente	994	0.623	4178	0.72×10^{-3}	7.24×10^{-7}	1.5×10^{-7}	4.83
Frio	1067.5	0.3799	3300	3.39×10^{-3}	2.4045×10^{-5}	1.08×10^{-7}	0.02
B Alumina	3050	30	618.3	-	-	-	-

2.1. Procedure for thermal analysis

$$\phi = 0.05\ fixed \tag{1}$$

$$Th_i = 98.0ºC\ fixed \tag{2}$$

$$Tc_i = 25.0ºC\ fixed \tag{3}$$

$$Re_h = 200\ fixed \tag{4}$$

$$Re_c = Re^* Re_h \tag{5}$$

ϕ is the volume fraction of the nanoparticles. Th_i and Tc_i are the inlet temperatures for hot and cold fluids, respectively. is the Reynolds number associated with the hot fluid and Re^* is the ratio of the Reynolds number of the cold fluid to the Reynolds number of the hot fluid.

$$Dh_C = \frac{4Ac_C Lf_C}{As_C} \tag{6}$$

Dh_C is the hydraulic diameter, $Ac_C = 42.2 \times 10^{-6}$ m² $Lf_C = 137 \times 10^{-3}$ m, $Lf_C = 137 \times 10^{-3}\ m$ is the channel length, $Asc = 34.716 \times 10^{-3}\ m^2$ is the heat transfer area for the cold fluid.

$$Dh_h = Dh_C \tag{7}$$

$$Lf_h = \frac{Dh_h As_h}{4Ac_h} \tag{8}$$

Lf_h is the channel length, $As_h = 26.037 \times 10^{-3}$ m² is the heat transfer area for the hot fluid.

The properties of the nanofluid are obtained by:

$$\rho_{nano} = \rho_{Particle}\phi + (1-\phi)\rho_C \tag{9}$$

$$\mu_{nano} = \frac{\mu_C}{(1-\phi)^{2.5}} \tag{10}$$

$$Cp_{nano} = \frac{Cp_{Particle}\rho_{Particle}\phi + (1-\phi)Cp_C\rho_C}{\rho_{nano}} \tag{11}$$

$$k_{nano} = \frac{[k_{Particle} + 2k_C + 2(k_{Particle} - k_C)(1-0.1)^3\phi]}{[k_{Particle} + 2k_C + 2(k_{Particle} - k_C)(1-0.1)^2\phi)}]K_c \tag{12}$$

$$\nu_{nano} = \frac{\mu_{nano}}{\rho_{nano}} \tag{13}$$

$$\alpha_{nano} = \frac{k_{nano}}{\rho_{nano} Cp_{nano}} \tag{14}$$

$$Pr_{nano} = \frac{\mu_{nano}}{\alpha_{nano}} \tag{15}$$

$$\mu_W = \frac{\mu_{nnao} + \mu_h}{2} \tag{16}$$

μ_W is the assumed value for the fluid's viscosity at the channel wall.

$$h_{nano} = 0.1706\ 6^{0.44}\ {Re_{nano}}^{0.324}\ {Pr_{nano}}^{\frac{1}{3}} \left(\frac{\mu_{nano}}{\mu_W}\right)^{0.14} \left(\frac{k_{nano}}{Dh_C}\right) \tag{17}$$

$$h_h = 0.1729\ 5^{0.44}\ {Re_h}^{0.324}\ {Pr_h}^{1/3} \left(\frac{\mu_h}{\mu_W}\right)^{0.14} \left(\frac{k_h}{Dh_h}\right) \tag{18}$$

The heat transfer coefficients of both fluids, cold (h_{nano}) and hot (h_h), were obtained by regression fit[4].

$$A_{Med} = \frac{As_h + As_C}{2} \tag{19}$$

The overall heat transfer coefficient is obtained by:

$$UoA = \frac{1}{\frac{1}{h_h\ As_h} + \frac{1}{h_{nano}\ As_c} + \frac{L}{k_{Metal}\ A_{Med}}} \tag{20}$$

$k_{Metal} = 16.2\ W/(m\ K)$ is the thermal conductivity of the heat transfer plate and $L = 0.4 \times 10^{-3}\ m$ is the thickness between the cold and hot channels.

$$\dot{m}_h = \frac{Re_h\ \mu_h\ Ac_h}{Dh_h} \tag{21}$$

$$\dot{m}_{nano} = \frac{Re_{nano}\ \mu_{nano}\ Ac_C}{Dh_C} \tag{22}$$

$$\dot{m}^* = \frac{\dot{m}_{nano}}{\dot{m}_h} \tag{23}$$

$\dot{m}_h$ and $\dot{m}_{nano}$ are the mass flow rates of the hot and cold fluid, respectively.

$$C_h = \dot{m}_h\ Cp_h \tag{24}$$

$$C_{nano} = \dot{m}_{nano}\ Cp_{nano} \tag{25}$$

C_h and C_{nano} are the heat capacities of the hot and cold fluids, respectively.

$$C^* = \frac{C_{min}}{C_{max}} \tag{26}$$

where C_{min} is the minimum value between C_h and C_{nano}.

$$NTU = \frac{UoA}{C_{min}} \tag{27}$$

NTU is the number of thermal units associated with the heat exchanger.

$$Fa = \frac{NTU(1 - C^*)}{2} counter\ flow \tag{28}$$

$$Fa = \frac{NTU(1 + C^*)}{2} parallel\ flow \tag{29}$$

Fa is the fin analogy for heat exchanger[13,14].

$$\eta_T = \frac{tanh(Fa)}{Fa} \tag{29}$$

η_T is the thermal efficiency.

$$\varepsilon_T = \frac{1}{\frac{1}{\eta_T\, NTU} + \frac{1 + C^*}{2}} \tag{30}$$

ε_T is the thermal effectiveness.

$$\dot{Q}_{Max} = (Th_i - Tc_i)\, C_{min} \tag{31}$$

$\dot{Q}_{Max}$ is the maximum heat transfer rate for the situation under analysis.

$$\dot{Q} = \frac{(Th_i - Tc_i)\, C_{min}}{\frac{1}{\eta_T\, NTU} + \frac{1 + C^*}{2}} \tag{32}$$

$\dot{Q}$ is the actual rate of heat transfer.

The outlet temperatures for both fluids, Th_O and Tc_O, are obtained by:

$$Th_O = Th_i - \frac{\dot{Q}}{\dot{m}\, Cp_h} \tag{33}$$

$$Tc_O = Tc_i - \frac{\dot{Q}}{\dot{m}\, Cp_{nano}} \tag{34}$$

$$\sigma_T = \left(\frac{C_h}{C_{min}}\right) ln\left(\frac{Th_o}{Tc_i}\right) + \left(\frac{C_{nano}}{C_{min}}\right) ln\left(\frac{Tc_o}{Tc_i}\right) \tag{35}$$

σ_T is the thermal irreversibility of the heat exchanger.

2.2. Procedure for hydrodynamic analysis

$$D_P = 0.6 \times 10^{-3}\, m\, fixed \tag{36}$$

D_P is the diameter of the entrance port.

$$Gc = \frac{\dot{m}_c}{Ac_c} \tag{37}$$

$$Gh = \frac{\dot{m}_h}{Ac_h} \tag{38}$$

$$Gp_c = \frac{4\dot{m}_c}{\pi {D_P}^2} \tag{39}$$

$$Gp_h = \frac{4\dot{m}_h}{\pi {D_P}^2} \tag{40}$$

Gc and Gh are the mass fluxes of the cold and hot fluids, respectively. Gp_c and Gp_h are the mass flows through the portals.

$$fc_c = \frac{0.316}{Re_{nano}^{0.25}} \tag{41}$$

$$fc_h = \frac{0.316}{Re_h^{0.25}} \tag{41}$$

$$fc_{Exp} = \frac{1.3383}{Re_{nano}^{0.5003}} \tag{42}$$

$$fh_{Exp} = \frac{1.3383}{Re_h^{0.5003}} \tag{43}$$

fc_c and fc_h are the theoretical friction factors associated with hot and cold fluids; fc_{Exp} and fh_{Exp} are the experimental coefficients of friction[3].

$$\Delta P_c = \frac{4fc_c Lf_c Gc^2}{2Dh_c \rho_{nano}} \tag{44}$$

$$\Delta P_h = \frac{4fc_h Lf_h Gh^2}{2Dh_h \rho_h} \tag{45}$$

$$\Delta P_{Pc} = \frac{1.5Gp_c{}^2}{2\rho_{nano}} \tag{46}$$

$$\Delta P_{Ph} = \frac{1.5Gp_h{}^2}{2\rho_h} \tag{47}$$

ΔP_c and ΔP_h are the pressure drops along the channels; ΔP_{Pc} and ΔP_{Ph} are the pressure drops in the portals.

$$P_{2c} = Patm\ assumed \tag{48}$$

$$P_{2h} = Patm\ assumed \tag{49}$$

$$P_{1c} = \Delta P_c + \Delta P_{Pc} + P_{2c} \tag{50}$$

$$P_{1h} = \Delta P_h + \Delta P_{Ph} + P_{2h} \tag{51}$$

$$\sigma_f = -\left(\frac{C_h}{C_{min}}\right) Rln\left(\frac{P_{2h}}{P_{1h}}\right) - \left(\frac{C_{nano}}{C_{min}}\right) Rln\left(\frac{P_{2c}}{P_{1c}}\right) \tag{52}$$

$$R = \frac{Th_i - Th_o}{Tc_o - Tc_i} \tag{53}$$

then:

$$\dot{S}_{genf} = \sigma_f C_{min} \tag{54}$$

σ_f and $\dot{S}_{genf}$ are the viscous irreversibility and the entropy generation rate[12].
finally:

$$Be = \frac{\dot{S}_{genT}}{\dot{S}_{genT+\dot{S}_{genf}}} \tag{55}$$

Be is the thermodynamic Bejan number[14–16].

3. Results and discussion

Figure 1 shows the relationships between the mass flows of fluids within the working range between them. The hot fluid flow corresponds to a fixed Reynolds number equal to 200, and the coolant flow corresponds to a variation for the Reynolds number between 50 and 1000. When you have ethylene glycol flowing with zero nanofluid mass fraction, the change in mass of the cold fluid is not significantly more significant when compared to the flow rate of the hot fluid. For Re_c= 1000, that is, Re^* = 5, the ratio between the masses of the cold fluid and the hot fluid is approximately equal to 20. However, when fractions of nanoparticles are included, the mass flow increases significantly with the increase in the number of nanoparticles. Reynolds is associated with soda. When Re_{nano} = 200, i.e., Re^* = 1, the nanofluid mass flow rate approximately corresponds to the ethylene glycol mass flow rate for Re^* = 5. This increase in mass flow significantly affects all parameters that will be analyzed in the context of this work.

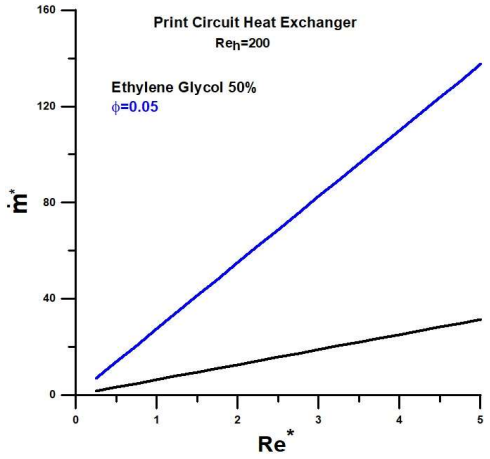

Figure 1. Ratio of mass flow rates of the cold fluid to the hot fluid.

Figure 2 shows the variation in the number of thermal units associated with the heat exchanger for the two situations under analysis: a flow of 50% pure ethylene glycol and a flow of 50% ethylene glycol plus 0.05 volume fraction Alumina Boehmite nanoparticles. For low flow rates of the refrigerant fluid, a significant increase in the number of thermal units of the nanofluid can be observed compared to the number of thermal units of the 50% pure ethylene glycol. However, the initial difference becomes less pronounced for high flow rates of the refrigerant fluid, tending to a limit value when $Re^* = 5$. The same occurs with the relationship between the thermal capacities of both fluids, **Figure 3**, with a significant difference for low flows and a slight difference for higher flows. These two parameters, NTU and C*, are primarily responsible for determining the thermal efficiency of the heat exchanger, as defined in this work.

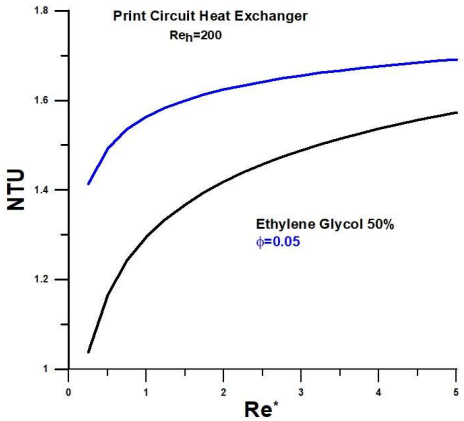

Figure 2. Number of thermal units (NTU) versus the ratio of Reynolds numbers.

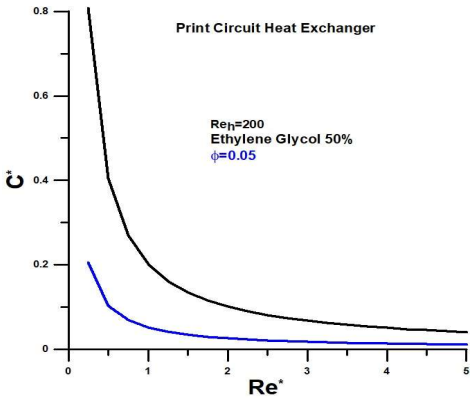

Figure 3. Ratio of heat capacities versus the ratio of Reynolds numbers.

The thermal efficiency of the heat exchanger is shown in **Figure 4**. In this context, the thermal efficiency represents the potential for heat exchange between the fluids. When the efficiency approaches 1, there is the maximum potential for heat exchange. After that, the heat exchange between the fluids tends to a minimum value, and this potential tends to zero. For example, there is a high heat exchange potential for 50% ethylene glycol at low refrigerant flow rates and an approximate 10% drop for nanofluid at a volume fraction equal to 0.05. It can be anticipated, in this case, that the potential presented by ethylene glycol was better used when introducing nanoparticles.

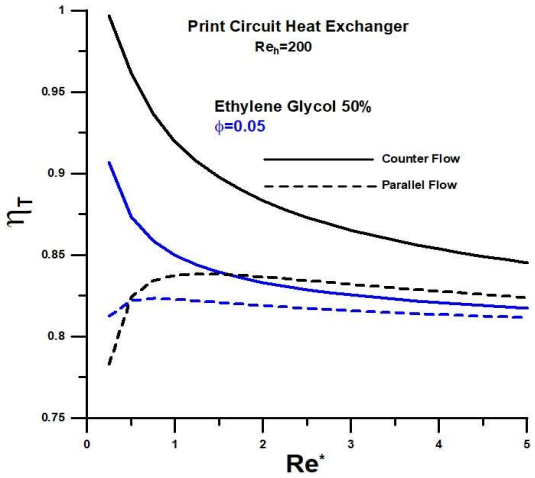

Figure 4. Thermal efficiency of the heat exchanger versus the ratio of Reynolds numbers.

When comparing the relationship between the heat transfer rates, represented by the thermal effectiveness, **Figure 5** shows that the heat transfer rate associated with the nanofluid is higher than that of ethylene glycol by 50%. In this case, it is observed again that the greatest difference occurs for lower refrigerant flows. For the lowest flow rate of the refrigerant, there is an approximate increase of 27% in the heat transfer rate when adding the nanofluid, and this value drops to approximately 6% for high flow rates. Regarding the two heat exchanger configurations under analysis, counterflow and parallel flow, it is evident that there is greater heat exchange for the counterflow type exchanger.

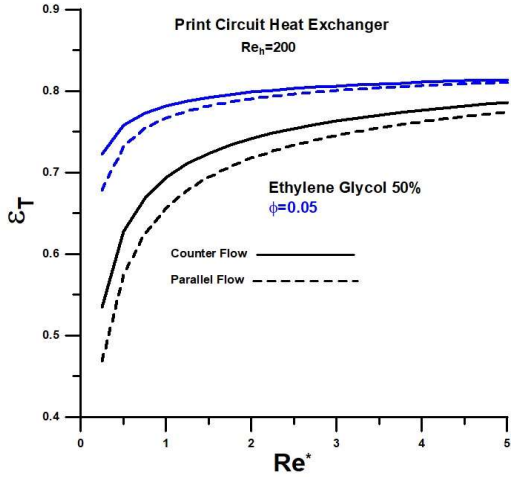

Figure 5. Thermal effectiveness of the heat exchanger versus the ratio of Reynolds numbers.

The thermal effectiveness of the heat exchanger is very similar to what is observed for the thermal irreversibility, as shown in **Figure 6**, making it evident that these are equivalent quantities when comparing the thermal performance of the heat exchanger.

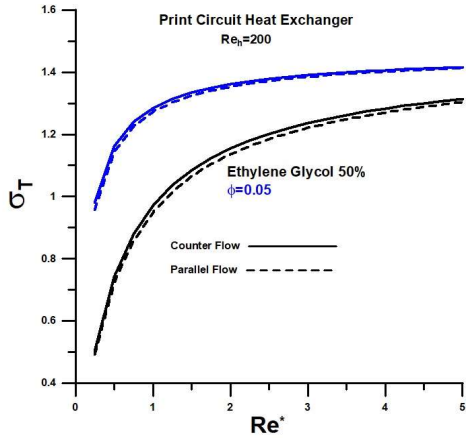

Figure 6. Thermal irreversibility versus the ratio of Reynolds numbers.

Regarding the last two analyzed quantities, thermal effectiveness and thermal irreversibility, it should be noted that none of them makes it possible to determine the absolute value of the heat transfer rate that occurs during the exchange process between fluids. Instead, they only indicate how close or far away the heat transfer rate is concerning the maximum possible heat transfer rate.

For a systemic analysis of the heat exchanger, considering quantities related to heat exchange and viscous dissipation, it becomes relevant to determine quantities associated with hydrodynamic aspects. The most pertinent parameter related to the flow is the friction factor. Just as the Nusselt number modulates the heat transfer, it effectively determines the pressure drop in the flow. **Figure 7** presents theoretical and empirical results for the friction factor for comparison purposes. The empirical correlation was obtained through experimental results determined by Rosa et al.[3] and the theoretical expression presented by Zhao et al.[8]. In this work, we chose to use empirical correlation to determine the magnitudes dependent on the friction factor since the results obtained experimentally are within the Reynolds numbers of the designed device.

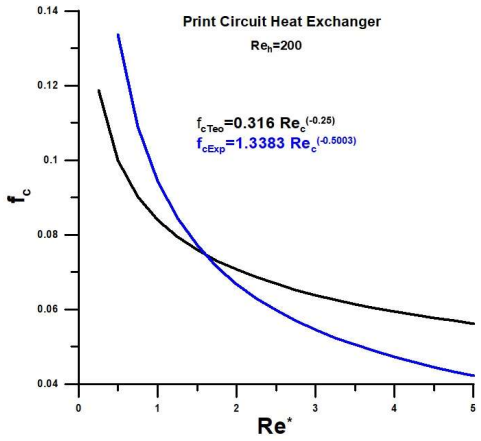

Figure 7. Theoretical and empirical friction factor versus the ratio of Reynolds numbers.

The viscous irreversibility is represented in **Figure 8**, as a function of the refrigerant fluid flow, with and without the inclusion of nanoparticles fraction. As already observed, when fractions of nanoparticle are included in the flow, the mass flow increases, significantly affecting the viscous irreversibility. In this particular case, the addition is exceptionally high for higher flows, preliminarily indicating the impossibility of working at the upper limit of flows for the refrigerant. At lower flow rates, however, the viscous dissipation added by the nanoparticles is of the same order of magnitude as the viscous dissipation

caused by 50% pure ethylene glycol. Therefore, it is expected that nanoparticles can be used for lower refrigerant flow rates.

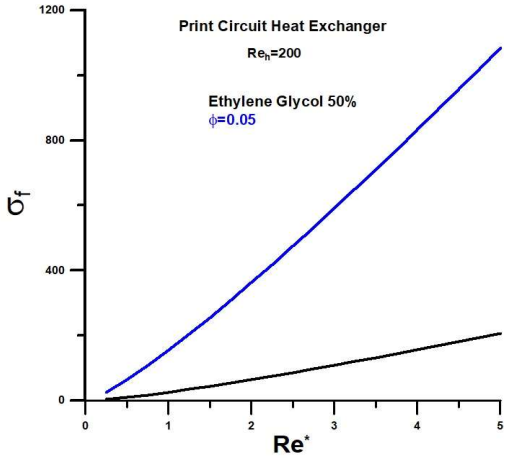

Figure 8. Viscous irreversibility versus the ratio of Reynolds numbers.

The ratio between thermal irreversibility and total irreversibility is represented in **Figure 9** through the Bejan thermodynamic number for a counterflow heat exchanger. At lower flow rates for the refrigerant, the thermal irreversibility is of the order of magnitude of the total irreversibility, which indicates a non-prevalence of viscous irreversibility. However, with the increase in the flow rate for the refrigerant, the Bejan number presents shallow values. It tends to a minimum value at medium and high flows, with significant relevance for the nanofluid concerning 50% pure ethylene glycol.

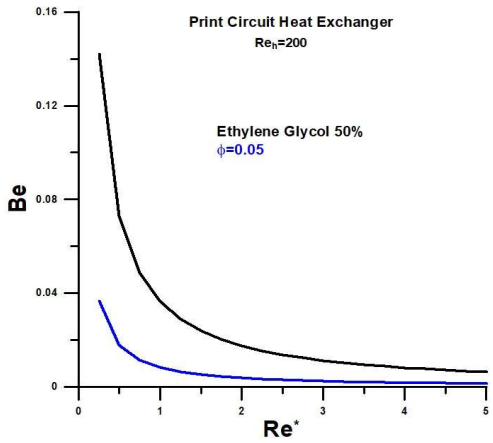

Figure 9. Bejan thermodynamic number versus the ratio of Reynolds numbers.

The data show that the heat exchanger should not work in the upper flow rate range for the refrigerant for a favorable cost-benefit ratio. However, the reasonable flow limit for 50% pure ethylene glycol is higher than the practical flow limit for the nanofluid. Preliminarily, based on the Bejan number, the threshold value for the Reynolds number in ethylene glycol is approximately equal to Re* = 3, and for the nanofluid, Re* = 1 is a probable indicator.

Figure 10 shows the relationship between the hot fluid outlet temperatures between nanofluid and 50% ethylene glycol. For lower flow rates, the outlet temperature for nanofluid is between 0.76 and 0.86 of the outlet temperature for 50% ethylene glycol for both counterflow and parallel flow configurations. For high flow rates, the ratio tends to be one, and, in this situation, there is no advantage in using

nanoparticles. However, **Figure 10** does not indicate the absolute values of the outlet temperatures for the hot fluid.

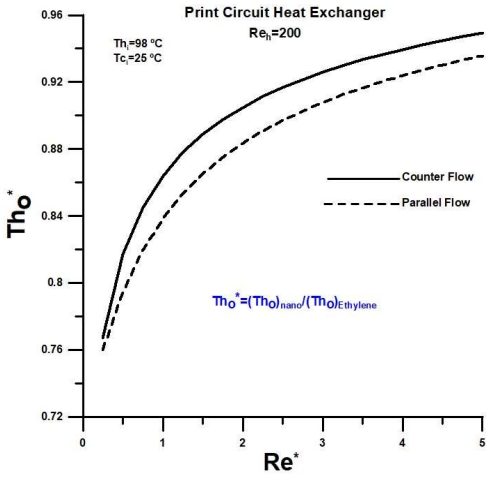

Figure 10. Hot fluid outlet temperatures ratio versus the ratio of Reynolds numbers.

The absolute values for the hot fluid outlet temperatures, when Reh = 200, are represented in **Figure 11**. The results obtained corroborate the previous conclusions and allow a decision of the flow ranges where a cost-benefit ratio is advantageous. For low flows, the temperature drop is significant. Still, from a given value, the decrease in temperature is negligible and does not justify the effort and energy consumption in the form of viscous dissipation. Therefore, we indicate again that the justifiable threshold flow for nanofluid corresponds to approximately Re* = 1, and for 50% pure ethylene glycol, Re* = 3 is a reasonable threshold value.

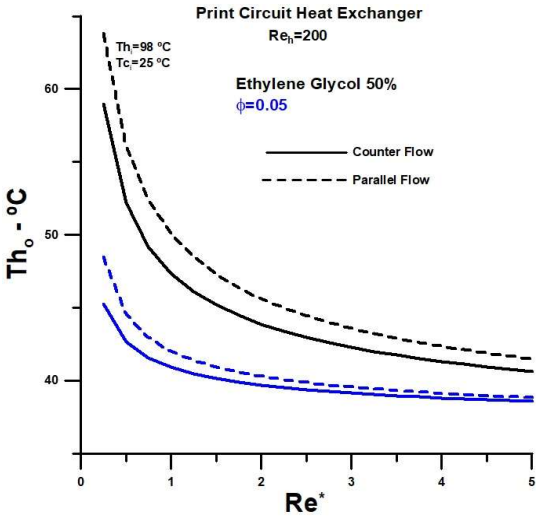

Figure 11. Hot fluid outlet temperatures for Reh = 200 versus the ratio of Reynolds numbers.

4. Conclusion

The work presents results from applying a dimensionless theory that uses the concepts of thermal efficiency in heat exchangers and quantities associated with the second law of thermodynamics. Thermohydraulic performance analysis was performed on a straight microchannel printed circuit heat exchanger. Counter-flow and parallel-flow configurations were analyzed for water cooling using 50% ethylene glycol base fluid and platelet-shaped non-spherical Boehmite Alumina nanoparticles.

The heat exchanger was designed to work in a range of Reynolds numbers between 200 and 850. However, high values for the Reynolds number increase viscous dissipation and lead to a degradation of the thermal potential, which is amplified with the inclusion of nanoparticles.

It is concluded that the heat exchanger under analysis must operate at low flow rates for the refrigerant fluid, where the potential for heat exchange remains high and reasonably above a minimum threshold. For lower refrigerant flows, viscous irreversibilities are relatively low concerning thermal irreversibilities, allowing a viable cost-benefit for the heat exchanger even with nanoparticles at a volume fraction equal to 5.0%.

It is proven that what should act to improve the thermal performance of the heat exchanger works in the sense of increasing viscous dissipations.

It is shown that the dimensionless analysis of heat exchangers, in the form presented, is a valuable tool for thermo-hydraulic optimization of heat exchangers.

5. List of symbols

Asc—the heat transfer area for the cold fluid, $[m^2]$

As_h—the eat transfer area for the hot fluid, $[m^2]$

A_{cc}—channel cross-sectional free flow area, $[m^2]$

Cp_c—specific heat of the cold fluid, $[\frac{J}{kg\,K}]$

Cp_h—specific heat of the hot fluid, $[\frac{J}{kg\,K}]$

Cp_{nano}—thermal capacity of the nanofluid, $[\frac{W}{K}]$

C_{min}—minimum thermal capacity between the hot and cold fluids, $[\frac{W}{K}]$

$$C^* = \frac{C_{min}}{C_{max}}$$

D_h—hydraulic diameter, $[m]$

D_P—port diameter, $[m]$

Fa—fin analogy for heat exchanger

Gc and Gh are the mass fluxes of the cold and hot fluids, respectively. Gp_c and Gp_h are the mass flows through the portals.

Gc—mass velocity of the cold fluid, $[\frac{kg}{m^2 s}]$

Gh—mass velocity of the hot fluid, $[\frac{kg}{m^2 s}]$

Gp_c—cold mass flows through the portal, $[\frac{kg}{m^2 s}]$

Gp_h—hot mass flows through the portal, $[\frac{kg}{m^2 s}]$

h_h—coefficient of heat convection for hot fluid, $[\frac{W}{m^2 K}]$

h_c—coefficient of heat convection for cold fluid, $[\frac{W}{m^2 K}]$

h_{nano}—coefficient of heat convection for nanofluid, $[\frac{W}{m^2 K}]$

k_h—thermal conductivity of the hot fluid, $[\frac{W}{m\,K}]$

k_c—thermal conductivity of the cold fluid, $[\frac{W}{m\,K}]$

k_{nano}—thermal conductivity of the nanofluid, $[\frac{W}{m\,K}]$

$\dot{m}_c$—total mass flow rate of the cold fluid, $[\frac{kg}{s}]$

$\dot{m}_h$—total mass flow rate of the hot fluid, $[\frac{kg}{s}]$

Pr_{nano}—is the Prandtl number of the nanofluid

$\dot{Q}$—actual heat transfer rate, $[W]$

$\dot{Q}_{max}$—maximum heat transfer rate, $[W]$

Re_c—Reynolds number for cold fluid

Re_h—Reynolds number for hot fluid

Tc_i—inlet temperatures of water, $[ºC]$

Th_i—inlet temperatures of vegetable oil, $[ºC]$

Tc_o—outlet temperatures for cold fluid, $[ºC]$

Th_o—outlet temperatures for hot fluid, $[ºC]$

Uo—global heat transfer coefficient, $[\frac{W}{m^2\,K}]$

UoA—overall heat transfer coefficient

Greek symbols

α_{nano}—thermal diffusivity of the nanofluid, $[\frac{m^2}{s}]$

ρ_{nano}—density of the nanofluid, $[\frac{kg}{m^3}]$

μ_{nano}—dynamic viscosity of nanofluid, $[\frac{kg}{m^3}]$

υ_{nano}—is the kinematic viscosity of the cold fluid, $[\frac{kg}{m^3}]$

ε_T—thermal effectiveness

η_T—thermal efficiency

Acronyms

NTU—number of thermal units

Author contributions

Conceptualization, EN; methodology, EN; software, EN; validation, EN; formal analysis, EN; investigation, EN; resources, EN; data curation, EN; writing—original draft preparation, EN; writing—review & editing, EN and HAM; visualization, HAM; supervision, HAM.

Conflict of interest

The authors declare no conflict of interest.

Reference

1. Nogueira É, Machado HA. Thermal efficiency and second law of thermodynamics applied in a straight microchannel printed circuit heat exchanger. In: Proceedings of the 19th Brazilian Congress of Thermal Sciences and Engineering (ENCIT 2022); 6–10 November 2022; Bento Gonçalves-RS, Brazil.
2. Seo JW, Kim YH, Kim D, et al. Heat transfer and pressure drop characteristics in straight microchannel of printed circuit heat exchangers. *Entropy* 2015; 17: 3438–3457. doi: 10.3390/e17053438
3. Rosa P, Karayiannis TG, Collins MW. Single-phase heat transfer in microchannels: The importance of scaling effects. *Applied Thermal Engineering* 2009; 29(17–18): 3447–3468. doi: 10.1016/j.applthermaleng.2009.05.015
4. Steinke ME, Kandlikar SG. Single-phase liquid heat transfer in microchannels. In: Proceedings of ICMM2005 3rd International Conference on Microchannels and Mini channel; 13–15 June 2005; Toronto, Canada. pp. 667–678.
5. Katz A, Aakre SR, Anderson MH, Ranjan D. Experimental investigation of pressure drop and heat transfer in high-temperature supercritical CO_2 and helium in a printed-circuit heat exchanger. *International Journal of Heat and Mass Transfer* 2021; 171: 121089. doi: 10.1016/j.ijheatmasstransfer.2021.121089
6. Baik SJ, Kim SG, Son SM, Lee JI. Printed circuit heat exchanger design, analysis and experiment. In: Proceedings of the 16th International Topical Meeting on Nuclear Reactor Thermal Hydraulics (NURETH-16); 30 August–4 September 2015; Chicago, United States.
7. Chai L, Tassou SA. A review of printed circuit heat exchangers for helium and supercritical CO_2 Brayton cycles. *Thermal Science and Engineering Progress* 2020; 18: 100543. doi: 10.1016/j.tsep.2020.100543
8. Zhao Z, Zhou Y, Ma X, et al. Numerical study on thermal hydraulic performance of supercritical LNG in zigzag-type channel PCHEs. *Energies* 2019; 12(3): 548. doi: 10.3390/en12030548
9. Bhosale SS, Acharya AR. Review on applications of micro-channel heat exchanger. *International Research Journal of Engineering and Technology* 2020; 7(3).
10. Tang LH, Yang BH, Pan J, Sundén B. Thermal performance analysis in a zigzag channel printed circuit heat exchanger under different conditions. *Heat Transfer Engineering* 2022; 43(7): 567–583. doi: 10.1080/01457632.2021.1896832
11. Timofeeva EV, Routbort JL, Singh D. Particle shape effects on thermophysical properties of alumina nanofluids. *Journal of Applied Physics* 2009; 106(1): 014304. doi: 10.1063/1.3155999
12. Monfared M, Shahsavar A, Bahrebar MR. Second law analysis of turbulent convection flow of Boehmite alumina nanofluid inside a double-pipe heat exchanger considering various shapes for nanoparticle. *Journal of Thermal Analysis and Calorimetry* 2019; 135(2): 1521–1532. doi: 10.1007/s10973-018-7708-7
13. Nogueira É. Influence of nanoparticles shapes of Boehmite alumina on the thermal performance of a straight microchannel printed circuit heat exchanger. *Journal of Metallic Material Research* 2022; 5(1): 8–24. doi: 10.30564/jmmr.v5i1.4364
14. Bejan A. The thermodynamic design of heat and mass transfer processes and devices. *International Journal of Heat and Fluid Flow* 1987; 8(4): 258–276. doi: 10.1016/0142-727X(87)90062-2
15. Fakheri A. Heat exchanger efficiency. *Journal of Heat Transfer* 2007; 129(9): 1268–1276. doi: 10.1115/1.2739620
16. Nogueira E. Thermal performance in heat exchangers by the irreversibility, effectiveness, and efficiency concepts using nanofluids. *Journal of Engineering Sciences* 2020; 7(2): F1–F7. doi: 10.21272/jes.2020.7(2).f1